TCA manuscript No.
(will be inserted by the editor)

Search of Manifolds of Nonsymmetric Valley-Ridge Inflection Points on the Potential Energy Surface of HCN

Benjamin Schmidt · Wolfgang Quapp

October 17, 2012

Abstract The potential energy surface of a chemical reaction contains Valley-Ridge inflection points (VRI) if – an often occurring phenomenon – the reaction path branches. In this paper, we introduce a new direct search method to detect these VRI points. It is based on an inductive execution of Gauss-Newton steps. Thus, for the first time we were able to find not only singular nonsymmetric VRI points, but whole VRI manifolds on the potential energy surface of HCN.

Keywords Potential Energy Surface · Valley-Ridge Inflection Point · Bifurcation of Reaction Paths · Manifold of VRIs

1 Introduction

The concept of the Minimum-Energy-Path (MEP) serves as a basic model to understand the process of chemical reactions. It is based on the Transition State Theory (TST) according to which reactants and products are energetically stable states, separated from each other by a potential barrier [1]. In the course of the reaction it is necessary to overcome the barrier.

From a mathematical point of view we treat reactants and products of a chemical reaction as minima on a Potential Energy Surface (PES). We then understand the MEP as a curve in the configuration space of the PES – a curve, which connects the two minima with a saddle point that corresponds to the potential barrier. Minima and saddle points on a PES are also called stationary points.

At this point it should be emphasized that the MEP is an "artificial chemical tool" [2] whose advantages lie in overcoming the following dimensionality problem: The PES geometry of an N-atomic molecule is described by $3N$ coordinates. By using internal coordinates the dimensionality can be reduced to $3N-6$. However, the PES of a molecule with more than four atoms is not wholly accessible. Instead, we determine a one-dimensional curve as a reaction path via MEP-concept.

Firstly it must be required that along the MEP the potential energy is strictly monotonic increasing from the reactant minimum to the saddle point and strictly monotonic decreasing from the saddle point to the product minimum. Secondly the MEP should take course through a valley on its way up to the saddle point. In mathematical terms the minimum energy path cannot be described more precisely. Paths which satisfy both conditions must be considered equally. This looseness leads to several reaction path models.

As the simplest and most commonly used model serves the steepest descent from the saddle point [3] which is the basis for Fukui's Intrinsic Reaction Coordinate (IRC) [4]. It meets the monotony demand but does not distinguish between valley- and ridge-structures on the PES [5].

A second reaction path model, the Gradient Extremal (GE) [6,7,8,9,10,11], yields curves that may proceed on the valley floor. Along GE-curves the gradient is an eigenvector of the Hessian. However, their determination is expensive. Moreover, valleys might end abruptly on the PES which leads to GE-curves being interrupted by turning points [12].

B. Schmidt
Rabet 36, 04315 Leipzig, Germany,
E-mail: schmidt_benjamin@arcor.de

W. Quapp
Mathematisches Institut, Universitï¿½t Leipzig, PF 100920, 04009 Leipzig, Germany,
E-mail: quapp@uni-leipzig.de,
Web: http://www.mathematik.uni-leipzig.de/MI/∼quapp

The Reduced-Gradient-Following method (RGF) [13, 14,15,16] has been proven as a very capable reaction path model. Along RGF-curves the gradient constantly points to one fixed search direction. Due to their equivalence to the continuous Newton method RGF-curves are also called Newton trajectories (NT). Normally they connect several minima and saddle points with each other. Their behaviour in case of reaction path branchings argues for RGF-curves as well. However, not necessarily any choice of a search direction leads to appropriate reaction paths since there are examples of non-monotone NTs and NTs containing turning points.

During certain chemical reactions branchings can occur. For example, one transition state (TS) might lead to two products in case the MEP bifurcates between TS and products. In this case several MEPs share the same transition structure. But for our calculations it is irrelevant whether the MEP bifurcates before, nearby or after the TS.

With the following considerations we can show that reaction path branchings take place independently of the chosen reaction path model: If the MEP proceeds along a valley the trajectory is bound to the valley floor, making the path stable. If, however, the valley turns into a ridge we obtain an instable path. Small changes of the trajectory lead to great deflections. The valley divides into two valleys and a ridge in between. Other kinds of splits are possible, too; cf. monkey-saddles [17], mixed-type VRIs or ridge-ridge inflections [18,19]. Points where this occurs are called Valley-Ridge Inflection points (VRI). They are specific points on the PES, independent of the chosen reaction path model [17]. The term "point" is deceptive though because VRI points might form an up to $(n-2)$-dimensional manifold in the configuration space of an n-dimensional PES [20,21]. The interest in determining VRI points has increased steadily over the past years [22,23,24].

The IRC is not fitted to find (nonsymmetric) VRI points. It results from a solution of a differential equation system which determines a tangent in gradient direction. Hence, IRC-curves are unique and free of bifurcations outside of stationary points [25]. At this point we want to emphasize that despite it is widely common to consider the IRC as minimum energy path, no reaction path branching can be truly described by following it [26,25]. Gradient Extremals are better fitted because GE-curves lead through VRI points [11] but usually don't bifurcate there. Besides their suitability as a reaction path model Newton trajectories have the nice property that they bifurcate at VRI points [27]. A so-called singular NT connects the VRI point with its adjacent stationary points. For its determination variational methods were used lately [28,29,30].

Finding VRI points or, if existing, whole VRI manifolds is this paper's objective. To achieve that we no longer use the property that VRI points are bifurcation points of singular Newton trajectories. Instead we directly calculate them with the help of an adjusted Gauss-Newton-step. In Section 2 we will explain the properties of VRI points and introduce the method we developed to find them. Basic principles of the method's implementation will be illustrated in Section 3 while Section 4 will show the method's results on the potential energy surface of HCN. For VRI points in a symmetry plane of the molecule, manifolds of such points are known already [27,31,32]. However, it is the first time that not only singular nonsymmetric VRI points were found but whole curves of such points.

2 Gauss-Newton step for VRI points

In the past, VRI points were mostly determined either in their capacity as bifurcation points of singular Newton trajectories [27,31,33] or via variational methods [28,34]. In contrast, we now introduce a direct search method. Therefore some theory must be gathered.

2.1 Calculating on potential energy surfaces

As mentioned above, an abstract idea of the potential energy surface meets our requirements. We assume that the PES is given by a scalar function of the molecule's coordinates in every point of interest. This leads to the following definition:

Definition Let K be a subset of the $\mathbb{R}^n$. Then we call the mapping $E : K \to \mathbb{R}$ an n-dimensional potential energy surface. K is called configuration space of the potential energy surface E.

For practical reasons, we demand that E is at least three times differentiable. Furthermore we need the gradient and the Hessian for our calculations.

Definition Be $\mathbf{x} = (x_1, \ldots, x_n)^t \in K$. Then, the vector of the first derivatives $\mathbf{g} : K \to \mathbb{R}^n$ and the matrix of the second derivatives $\mathbf{H} : K \to \mathbb{R}^{n\times n}$ by

$$\mathbf{g}(\mathbf{x}) = \nabla E(\mathbf{x}) = \left(\frac{\partial E(\mathbf{x})}{\partial x_1}, \ldots, \frac{\partial E(\mathbf{x})}{\partial x_n} \right)^t,$$

$$\mathbf{H}(\mathbf{x}) = \nabla\nabla E(\mathbf{x}) = \left(\frac{\partial^2 E(\mathbf{x})}{\partial x_i \partial x_j} \right)_{\substack{i=1,\ldots,n \\ j=1,\ldots,n}}$$

are called gradient and Hessian of E.

The Hessian is symmetric. At stationary points (minima, saddle points) the gradient becomes (the) zero (vector). Finally, we define the adjoint matrix of $\mathbf{H}$.

Definition Be $\mathbf{H} \in \mathbb{R}^{n\times n}$ and let $\mathbf{H}^{ij} \in \mathbb{R}^{(n-1)\times(n-1)}$ be the matrix, that evolves from $\mathbf{H}$ by omitting the i-th row and the j-th column. If we set $\tilde{a}_{ij}$ according to

$$\tilde{a}_{ij} := (-1)^{i+j} \det\big(\mathbf{H}^{ij}\big),$$

then the matrix $\mathbf{A} := (\tilde{a}_{ji})_{\substack{j=1,\dots,n\\ i=1,\dots,n}}$ is called the adjoint matrix of $\mathbf{H}$. Note, that the indices i and j are interchanged.

The following relation holds between the Hessian and its adjoint matrix:

$$\mathbf{AH} = \det(\mathbf{H})\mathbf{I}_n, \tag{2.1}$$

where $\det(\mathbf{H})$ is the determinant of $\mathbf{H}$ and $\mathbf{I}_n$ is the n-dimensional unit matrix. Since (2.1) holds, $\mathbf{A}$ is sometimes named the desingularized inverse matrix of $\mathbf{H}$.

2.2 Properties of VRI points

If the minimum energy path is situated in a valley, then the eigenvalues corresponding to the Hessian's eigenvectors which are orthogonal to the gradient are positive. On its way up the valley an eigenvalue may become smaller until it is finally negative on a ridge. For this reason we obtain the following definition for VRI points:

Definition Let $\mathbf{x}$ be a non-stationary point in the configuration space of the PES, hence $\mathbf{g}(\mathbf{x}) \neq \mathbf{0}$. Let the eigenvalue which corresponds to one of the eigenvectors of $\mathbf{H}(\mathbf{x})$ which are orthogonal to $\mathbf{g}(\mathbf{x})$ be zero. Then $\mathbf{x}$ is called VRI point. Note, that we exclude VRI points which are also transition states, so-called monkey saddles [17].

Let $\mathbf{u}$ be the Hessian's eigenvector with the eigenvalue zero. Following the definition, we then have $\mathbf{g}^t\mathbf{u} = 0$ in VRI points. Through this, we get our first property:

Property 2.2.1 In VRI points $\mathbf{x} \in K$ the relation

$$\mathbf{A}(\mathbf{x})\mathbf{g}(\mathbf{x}) = \mathbf{0} \tag{2.2}$$

holds.

A proof is given in [27]. We want to briefly outline it. Let therefore $\mathbf{u}^i$ be the eigenvectors of $\mathbf{H}$ and λ_i the corresponding eigenvalues. Since $\lambda_i\mathbf{u}^i = \mathbf{H}\mathbf{u}^i$ holds, we obtain after multiplication with $\mathbf{A}$:

$$\lambda_i\mathbf{A}\mathbf{u}^i = \mathbf{A}\mathbf{H}\mathbf{u}^i \overset{(2.1)}{=} \det(\mathbf{H})\mathbf{u}^i = \left(\prod_{j=1}^{n}\lambda_j\right)\mathbf{u}^i.$$

In case of $\lambda_i \neq 0$ the adjoint $\mathbf{A}$ has eigenvectors $\mathbf{u}^i$ with corresponding eigenvalues $(\prod_{j=1}^n \lambda_j)/\lambda_i$. According to the VRI definition one eigenvalue of $\mathbf{x}$ equals zero, WLOG $\lambda_1 = 0$. Hence, the eigenvectors $\mathbf{u}^2, \dots, \mathbf{u}^n$ of $\mathbf{A}$ have the eigenvalue zero (as the product always equals zero). We write $\mathbf{g}$ as a linear combination of the $\mathbf{u}^i$ by $\mathbf{g} = \sum_{k=1}^n \xi_k\mathbf{u}^k$. Since in the VRI point $\mathbf{x}$ the gradient $\mathbf{g}$ is orthogonal to $\mathbf{u}^1$, it is $\xi_1 = 0$ and we obtain

$$\begin{aligned}\mathbf{A}(\mathbf{x})\mathbf{g}(\mathbf{x}) &= \mathbf{A}(\mathbf{x})\left(\sum_{k=1}^{n}\xi_k\mathbf{u}^k(\mathbf{x})\right)\\ &= \underbrace{\xi_1}_{=0}\mathbf{A}(\mathbf{x})\mathbf{u}^1(\mathbf{x}) + \sum_{k=2}^{n}\xi_k\mathbf{A}(\mathbf{x})\mathbf{u}^k(\mathbf{x})\\ &= \sum_{k=2}^{n}\xi_k\underbrace{\left(\frac{\prod_{j=1}^n\lambda_j}{\lambda_k}\right)}_{=0}\mathbf{u}^k(\mathbf{x}) = \mathbf{0}.\end{aligned}$$

Now that Property 2.2.1 is proven, a second one follows as a direct implication:

Property 2.2.2 Since VRI points $\mathbf{x} \in K$ are non-stationary, we have $\mathbf{g}(\mathbf{x}) \neq \mathbf{0}$. Combined with the property above, $\mathbf{A}(\mathbf{x})\mathbf{g}(\mathbf{x}) = \mathbf{0}$, it follows immediately that the kernel of $\mathbf{A}(\mathbf{x})$ is nontrivial. Hence we have

$$\det\mathbf{A}(\mathbf{x}) = 0. \tag{2.3}$$

Combining the two properties we realize that VRI points are the zeros of the mapping $f : K \to \mathbb{R}^{n+1}$ by

$$f(\mathbf{x}) := \begin{bmatrix}\mathbf{A}\mathbf{g}\\ \det\mathbf{A}\end{bmatrix}(\mathbf{x}). \tag{2.4}$$

It must be pointed out that f maps a point $\mathbf{x}$ of the configuration space to an $(n+1)$-dimensional vector. The first n components of $f(\mathbf{x})$ are identical with the components of $\mathbf{A}(\mathbf{x})\mathbf{g}(\mathbf{x})$ while the $(n+1)$-th component equals $\det\mathbf{A}(\mathbf{x})$.

It will be our objective to determine the zeros of f directly via a Gauss-Newton step. But prior to this we would like to show how VRI points and the desingularized continuous Newton method are interconnected.

2.3 VRI points and Newton's method

In its classic formulation Newton's method

$$\mathbf{x}^{j+1} := \mathbf{x}^j - \alpha\cdot\mathbf{H}\big(\mathbf{x}^j\big)^{-1}\mathbf{g}\big(\mathbf{x}^j\big)$$

converges under certain conditions to a zero of the gradient $\mathbf{g}$, in our case to a minimum or a saddle point. The starting point $\mathbf{x}^0$ must be suitably close to the stationary point and the step length α must be chosen suitably small. In the limiting case of infinitesimal step lengths we obtain Newton's continuous differential equation:

$$\dot{\mathbf{x}} = -\mathbf{H}(\mathbf{x})^{-1}\mathbf{g}(\mathbf{x})$$

When solving the equation above numerically we have to overcome the problems caused by the singularities of $\mathbf{H}$, hence all the points in which the right hand side of the equation is not defined. With the help of the adjoint matrix one changes over to the desingularized formulation and calls the method for solving

$$\dot{\mathbf{x}} = -\mathbf{A}(\mathbf{x})\mathbf{g}(\mathbf{x}) \tag{2.5}$$

the desingularized continuous Newton method. As (2.1) holds, the phase portraits of both differential equations are identical except for orientation [21]. The trajectories of (2.5) are called Newton trajectories (NT). As the gradient's direction remains constant along an NT, we can treat RGF-curves, which have been introduced as a reaction path model, as Newton trajectories as well.

We have to distinguish between two kinds of end points of the desingularized continuous Newton method:

(i) Points, where $\mathbf{g} = \mathbf{0}$ and $\mathbf{A}$ is nonsingular, are called essential singularities [35]. These are the stationary points on a PES. They are either attracting or repelling fixed points of (2.5). By change of sign one changes the fixed character of the point and with the help of Branin's equation

$$\dot{\mathbf{x}} = \pm\mathbf{A}(\mathbf{x})\mathbf{g}(\mathbf{x})$$

one can find a lot of (if not all) stationary points on the PES.

(ii) Points, where $\mathbf{Ag} = \mathbf{0}$ and $\mathbf{g} \neq \mathbf{0}$ hold, are called extraneous singularities [35]. According to (2.2) these are the VRI points. Following the argumentation in [20] the set of extraneous singularities of the desingularized continuous Newton method (and hence the set of VRI points) might be an up to $(n-2)$-dimensional closed subset of the configuration space $K \subset \mathbb{R}^n$. Thus, the term VRI *point* is deceptive. On symmetric subspaces of potential energy surfaces like the ones of water and formaldehyde whole VRI-curves were already found [31].

As VRI points might be parts of high-dimensional manifolds one must question their meaning. Is it *a* bifurcation point of *the* reaction path? Should the reaction path (minimum energy path) be defined as a singular curve on the PES whatsoever? These questions cannot be answered here. Nevertheless, they will need to be discussed.

2.4 A Gauss-Newton step [36,37,38]

Let us move on to the actual objective of this paper: Finding zeros of the mapping f defined by (2.4). Therefore, we define a generalized inverse matrix at first.

2.4.1 The Moore-Penrose pseudoinverse

Be $M \in \mathbb{R}^{p\times q}$. The matrix $M^+ \in \mathbb{R}^{q\times p}$ is called Moore-Penrose pseudoinverse of M, if the following conditions are fulfilled:

$$\begin{aligned} (M^+M)^t &= M^+M, & MM^+M &= M,\\ (MM^+)^t &= MM^+, & M^+MM^+ &= M^+. \end{aligned}$$

The Moore-Penrose inverse exists and is unique for any given matrix M. With its help, we can "invert" rectangular matrices.

2.4.2 Gauss-Newton step for VRI points

Now, all preparations are done and we can explain the method to determine zero vectors of the mapping f, defined by (2.4). Starting with $\mathbf{x} \in K$ we have to calculate $\Delta\mathbf{x}$, so that $\mathbf{x}+\Delta\mathbf{x}$ is a better approximation to the zero of f. Then, the Taylor series yields

$$f(\mathbf{x}+\Delta\mathbf{x}) = f(\mathbf{x}) + J_f(\mathbf{x})\cdot\Delta\mathbf{x} + O\big(\|\Delta\mathbf{x}\|_2^2\big)$$

where

$$J_f(\mathbf{x}) = \begin{pmatrix} \frac{\partial f_1(\mathbf{x})}{\partial x_1} & \cdots & \frac{\partial f_1(\mathbf{x})}{\partial x_n} \\ \vdots & \ddots & \vdots \\ \frac{\partial f_{n+1}(\mathbf{x})}{\partial x_1} & \cdots & \frac{\partial f_{n+1}(\mathbf{x})}{\partial x_n} \end{pmatrix}$$

is the Jacobian matrix of f. If we omit the terms of the second order and keep in mind that $f(\mathbf{x}+\Delta\mathbf{x}) \approx \mathbf{0}$ holds, we have

$$J_f(\mathbf{x})\cdot\Delta\mathbf{x} = -f(\mathbf{x}),$$

being a linear equation system, whose solutions may be used to gain better approximations to zeros of f. If we solve the term above using the Moore-Penrose pseudoinverse, we obtain

$$\Delta\mathbf{x} = -J_f(\mathbf{x})^+ f(\mathbf{x}). \tag{2.6}$$

In summary, we have shown that VRI points are the zeros of the mapping $f = \left[\begin{smallmatrix}\mathbf{Ag}\\ \det\mathbf{A}\end{smallmatrix}\right]$. Starting with $\mathbf{x}^0$ we iteratively determine them by

$$\mathbf{x}^{k+1} = \mathbf{x}^k + \Delta\mathbf{x}^k \overset{(2.6)}{=} \mathbf{x}^k - J_f(\mathbf{x}^k)^+ f(\mathbf{x}^k) \tag{2.7}$$

for $k = 0, 1, 2, \ldots$.

3 Comments on the implementation

Before explaining the actual program we would like to give some comments on the implementation of the Jacobian matrix and the Moore-Penrose pseudoinverse.

3.1 Implementing the Jacobian matrix

Let $\mathbf{x} \in K$ be a point of the configuration space of the PES. Then we approximate the partial derivative $\partial f_i/\partial x_j$ where $i = 1, \ldots, n+1$ and $j = 1, \ldots, n$ by a forward difference quotient

$$\frac{\partial f_i(\mathbf{x})}{\partial x_j} \approx \frac{f_i(\mathbf{x} + h \cdot \mathbf{e}_j) - f_i(\mathbf{x})}{h}, \tag{3.1}$$

where $h \in \mathbb{R}$ is still to be specified and $\mathbf{e}_j$ is the j-th unit vector of the $\mathbb{R}^n$.

The accuracy of the approximation essentially depends on the choice of h. On the one hand the disturbance $\mathbf{x} + h\mathbf{e}_j$ shall not be too small in case of $x_j \gg 1$. On the other hand we want to reduce the cancellation by not choosing h to be too small. In the latter case we had $|f_i(\mathbf{x} + h\mathbf{e}_j) - f_i(\mathbf{x})| \approx 0$. Thus, we set

$$h := \sqrt{\varepsilon} \cdot \max\{1, |x_j|\}$$

and choose $\varepsilon = 10^{-12}$.

It has to be considered that determining the Jacobian matrix is quite expensive because f must be determined at the $n+1$ points $\mathbf{x}$ and $\mathbf{x}^{r_j} := \mathbf{x} + h\mathbf{e}_j$, with $j = 1, \ldots, n$. In case of HCN four calls of f are necessary per program run.

3.2 Implementing the Moore-Penrose pseudoinverse

To obtain the Moore-Penrose pseudoinverse of a matrix $M \in \mathbb{R}^{p\times q}$ a singular value decomposition has to be carried out. Any matrix, where $p \geq q$ holds, can be written as a product

$$M = U \Sigma V^t$$

of an orthogonal matrix $U \in \mathbb{R}^{p\times q}$, a diagonal matrix $\Sigma = \operatorname{diag}(\sigma_1, \ldots, \sigma_q) \in \mathbb{R}^{q\times q}$ and the transposed of an orthogonal matrix $V \in \mathbb{R}^{q\times q}$. The σ_i are the eigenvalues of M. Then, we have

$$M^+ = V \Sigma^+ U^t,$$

where $\Sigma^+ = \operatorname{diag}(\tilde{\sigma_1}, \ldots, \tilde{\sigma_q})$ is a diagonal matrix with the entries

$$\tilde{\sigma_i} = \begin{cases} 1/\sigma_i & \text{, if } \sigma_i \neq 0 \\ 0 & \text{, else} \end{cases}$$

By (2.7) we have to determine the Moore-Penrose pseudoinverse of the Jacobian matrix $J_f(\mathbf{x})$. Thus, it holds $p = n+1$ and $q = n$. The source code for implementing the singular value decomposition is taken from [39].

3.3 Program for the detection of VRIs on the PES of HCN

The necessary calculations of gradient and Hessian are performed by Firefly Version 7.1.G (formerly PC-Gamess) [40]. We use the standard basis set 6-31G** with the following input file:

```
$CONTRL SCFTYP=rhf NZVAR=3   EXETYP=binv
        COORD=zmt  MAXIT=999 RUNTYP=optimize $END
$SYSTEM TIMLIM=5   MEMORY=400000             $END
$BASIS  GBASIS=N31 NGAUSS=6  NDFUNC=1        $END
$STATPT HESS=calc  NSTEP=1   DXMAX=0.00001
        NPRT=-2    NPUN=3                    $END
$FORCE  METHOD=analytic      PRTIFC=.true.   $END
```

The program is divided into four sections with Firefly being called between the second and the third subprogram. In detail, the following tasks are being executed:

(i) Providing the actual point $\mathbf{x}$ for iteration and providing the shifted points $\mathbf{x}^{r_j} := \mathbf{x} + h\mathbf{e}_j$ (with $j = 1, 2, 3$) for calculating the Jacobian matrix.
(ii) Providing the Firefly input for the four points $\mathbf{x}$ and $\mathbf{x}^{r_j}$, $j = 1, 2, 3$.
(iii) Call Firefly for gradient and Hessian.
(iv) Analysis of the Firefly output.
  (a) Reading out the gradient $\mathbf{g}$ and the Hessian $\mathbf{H}$
  (b) Calculating the adjoint matrix $\mathbf{A}$
  (c) Calculating the function $f = \left[\begin{smallmatrix} \mathbf{Ag} \\ \det \mathbf{A} \end{smallmatrix}\right]$. To calculate the determinant we use the LU-decomposition of $\mathbf{A}$ after the method of Crout [39].
(v) Actual iteration step.
  (a) Calculating the Jacobian matrix $J_f(\mathbf{x})$ and its Moore-Penrose pseudoinverse $J_f(\mathbf{x})^+$.
  (b) Calculating the iterated point $\mathbf{x}^{\text{new}}$ by (2.7):

$$\mathbf{x}^{\text{new}} = \mathbf{x} + \text{stl} \cdot \Delta\mathbf{x} = \mathbf{x} - \text{stl} \cdot J_f(\mathbf{x})^+ f(\mathbf{x}) \tag{3.2}$$

with a suitable step length $\text{stl} > 0$.

The subprograms (ii) and (iv) as well as Firefly itself have to be called four times per program run. This and the whole overriding control of all four subprograms plus the monitoring of the stop criterion is governed by a batch file.

4 Results

4.1 VRI-curves

In this section we consider points in the configuration space of the HCN potential energy surface to be vectors in terms of

$$\mathbf{x} = (r_{\mathrm{CH}}, r_{\mathrm{CN}}, \alpha)^t$$

where r_{CH} and r_{CN} are the distances C–H respectively C–N in Å and α is the angle between H–C–N in degree.

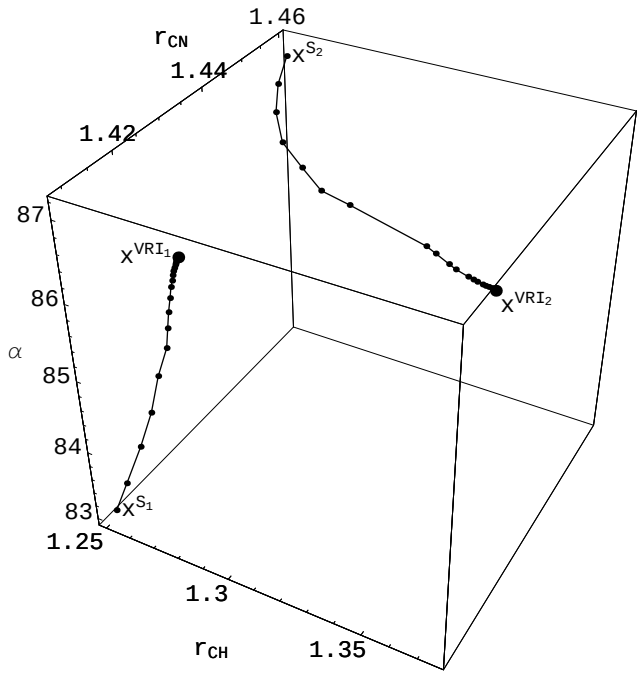

Fig. 4.1 Iteration steps that lead from the starting points $\mathbf{x}^{\mathrm{S}_1}$ and $\mathbf{x}^{\mathrm{S}_2}$ to the corresponding VRI points $\mathbf{x}^{\mathrm{VRI}_1}$ and $\mathbf{x}^{\mathrm{VRI}_2}$.

At first we want to examine the VRI points which occur when the N-atom dissociates from the saddle point. Therefore, we choose (arbitrarily, but nearby the already known VRI points [33,34]) two starting points $\mathbf{x}^{\mathrm{S}_1} = (1.25, 1.41, 83.)^t$ and $\mathbf{x}^{\mathrm{S}_2} = (1.25, 1.46, 87.)^t$. With a step length of stl = 0.25 and a suitable stop criterion, if $|\mathbf{Ag}| < 10^{-5}$, we subsequently obtain the two following VRI points after 45 iterations each:

$$\mathbf{x}^{\mathrm{VRI}_1} = (1.28324, 1.41188, 86.739)^t,$$
$$\mathbf{x}^{\mathrm{VRI}_2} = (1.37582, 1.41906, 87.001)^t$$

Figure 4.1 shows the single iteration steps from both starting points to the corresponding VRI points.

Since there are assumably more VRI points between the two we have already found, we put a straight chain of points between $\mathbf{x}^{\mathrm{VRI}_1}$ and $\mathbf{x}^{\mathrm{VRI}_2}$ which in turn we use as new starting points for the algorithm. In this way we obtain new VRI points, depicted in Figure 4.2.

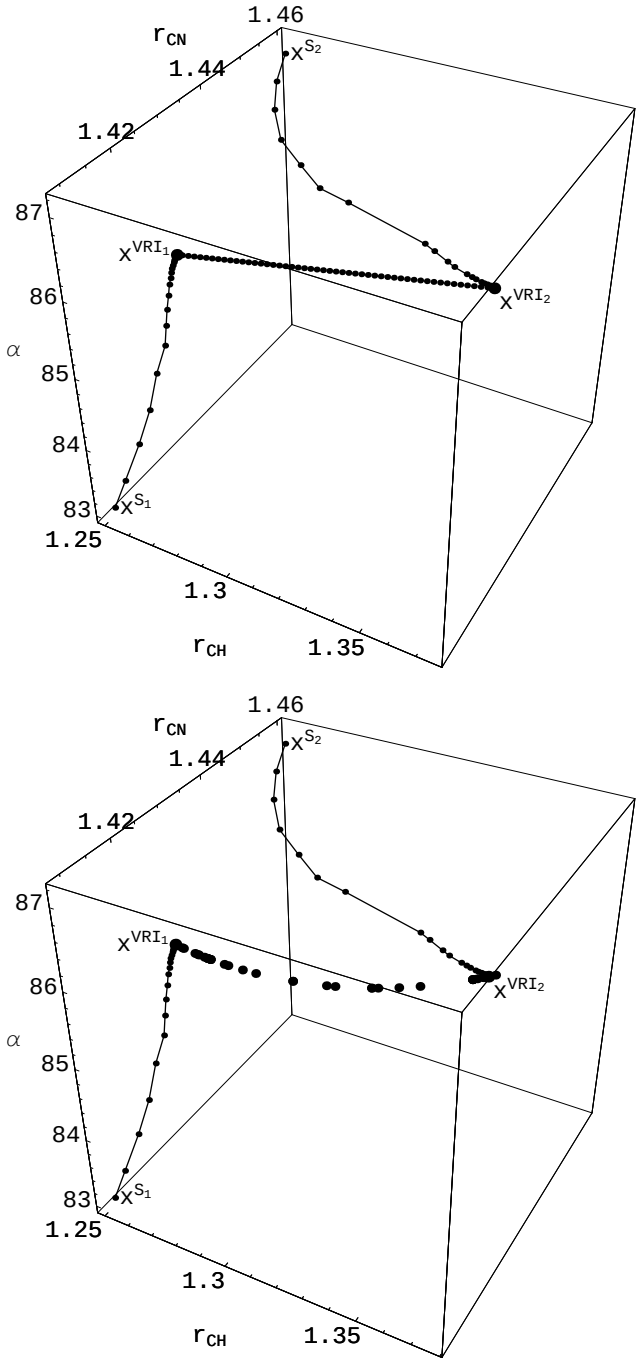

Fig. 4.2 A straight chain of starting points (above) lead to new VRI points (below).

By closing the gaps between the single VRI points successively and following the resulting curve over the end points $\mathbf{x}^{\mathrm{VRI}_1}$ and $\mathbf{x}^{\mathrm{VRI}_2}$ we obtain an even longer curve with end points in $(1.0212, 1.6751, 84.798)^t$ and $(1.5464, 1.4446, 103.65)^t$, as one can see in Figure 4.3.

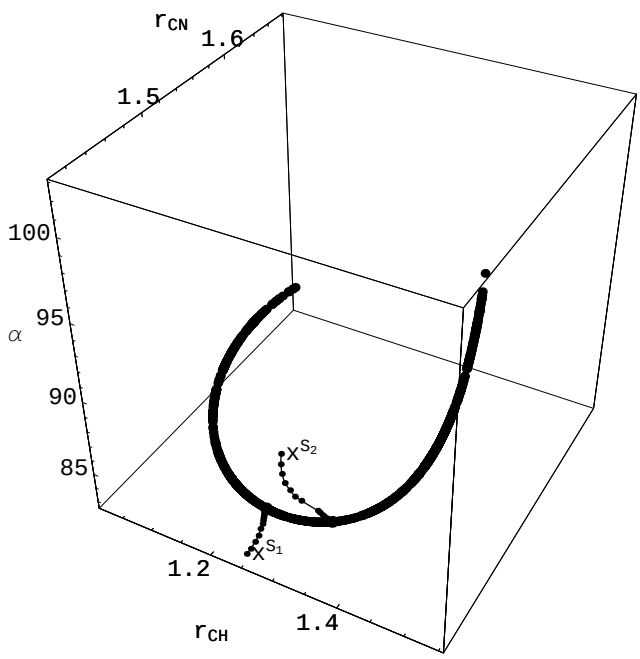

Fig. 4.3 VRI-curve when the N-atom leaves the transition structure

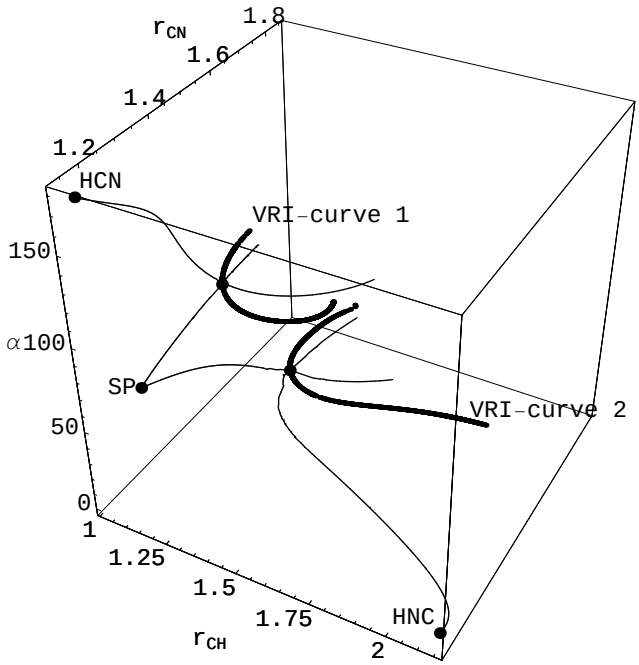

Fig. 4.4 Both VRI-curves (bold) with singular Newton trajectories (thin) through one VRI point of each curve. Analogous NT-branches emerge for all the other VRI points of the given curves.

A possible interpretation of this VRI curve would be the following: A dissociating N-atom leaves the saddle-point structure over a two-dimensional ridge. When meeting the VRI curve the N-atom has to decide whether to leave the ridge and dissociate completely along a valley, or to return to the minimum HCN through a valleys [34]. The fourth branch is a ridge leading into the PES mountains. Note, the VRI is of a mixed type. A valley touches a ridge. Figure 4.4 shows the VRI curve (VRI curve 1) with four RGF-branches at one of its VRI points and hence the possible paths for the N-atom to go along.

As a second example we want to detect VRI points on the pathway where the H-atom comes from the saddle point and meets the C≡N triple bond which is a saddle point of index 2. This case has already been analyzed, as well [34]. As the discovered VRI points lay very closely together, it was supposed even then that those points might be part of one curve. This can be proven now. Following the same procedure as described above, we started this time in the already known VRI points and were able to close the gaps between them by executing our algorithm.

Figure 4.4 shows the VRI-curve we obtained (VRI-curve 2) and exemplary the VRI point

$$\mathbf{x}^{\mathrm{VRI}} = (1.365, 1.468, 47.563)^t$$

with the four branches of the singular Newton trajectory that bifurcates in it. The curve's two end points are $(1.3096, 1.8040, 31.285)^t$ and $(2.0053, 1.5205, 43.192)^t$.

4.2 Singular Newton trajectories

Every VRI point belongs to a singular Newton trajectory which bifurcates in it. Since we found curves of VRI points there must be a family of singular NTs that hypersurfaceersurface" in the configuration space of the PES.

To determine the singular RGF-curves we use two approaches. The first one is based on the very same method we developed here for VRI-detection. Since it is basically a zero search we slightly adjust it to find the zeros of the projector equation

$$\mathbf{0} = \mathbf{P}_{\mathbf{r}}\mathbf{g}(\mathbf{x}) := \big(\mathbf{I}_n - \mathbf{r}\mathbf{r}^t\big)\mathbf{g}(\mathbf{x}). \tag{4.1}$$

All points $\mathbf{x}$ which fulfill the equation (4.1) form the Newton trajectory to the fixed search direction $\mathbf{r}$. If we identify $\mathbf{r}$ with the normalized gradient of one of the VRI points we will get the singular NT which bifurcates in that VRI point. Figure 4.4 shows the results for the VRI points $(1.1266, 1.4691, 87.545)^t$ and $(1.365, 1.468, 47.563)^t$.

However, in flat sections of the PES this method might cause trouble by jumping over the sought branch

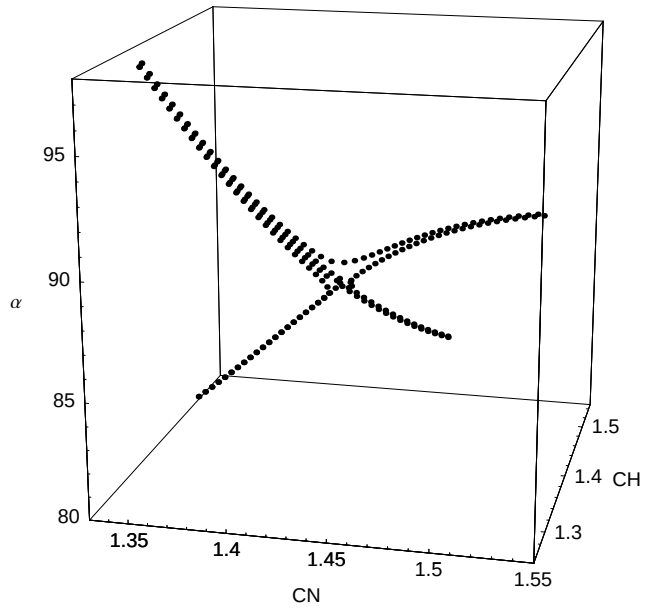

Fig. 4.5 Approximation of the four branches of a singular NT which were determined with Branin predictor steps by the iterative method of [34]. The corresponding VRI point is at the intersection at $(1.42, 1.44, 87.3)^t$

of the singular NT to another one. In that case we returned to the well-known predictor-corrector method [27,41] for determining RGF-curves. Usually, corrector steps did not work in these sections either. So we only used Branin predictor steps to determine the singular RGF-curves. Results can be seen in Figure 4.5 which shows the beginning of the four branches of a singular Newton trajectory.

5 Conclusions and outlook

It was our objective to develop a new direct search method for VRI points on the basis of the Gauss-Newton method. Valued at the results, this objective was achieved.

So far, VRI points were mostly considered as special singularities of the Newton method, meaning that one practically determined the corresponding singular Newton trajectory at first (by a "reasonable" guess or with variational treatment) and obtained the VRI point finally as its bifurcation point. This "detour" is not necessary here. With the introduced algorithm one has another method available to detect these special points of interest on a potential energy surface.

Beyond that, we succeeded in finding whole curves of nonsymmetric VRI points on the PES of HCN with this method's help. That is noteworthy insofar as now questions about the meaning of VRI points and thereby the meaning of the minimum energy path will arise again. Which one of the VRI-curve points corresponds to the reaction path branching? Can the reaction path be considered as a singular curve on the PES at all?

Additionally it must be emphasized that HCN (with its three atoms) is one of the smallest molecules where VRI manifolds with a dimension greater that zero might occur. And they do! It is very likely that potential energy surfaces of greater molecules do not only contain singular VRI points as found before but whole high-dimensional VRI manifolds. This will have to be examined as well.

It will certainly be our future work to applicate the method on different potential energy surfaces. As the basis of the method is a zero search it surely can be adjusted to determine steepest-descent curves or RGF-curves. For the latter ones the often used predictor-corrector method could be dropped when applying Gauss-Newton steps (3.2) iteratively instead, at least where the PES is not too flat.

References

1. H. Eyring and M. Polanyi. Über einfache Gasreaktionen. *Z physikal Chem*, B12:279–311, 1931.
2. D. Heidrich. An Introduction to the Nomenclature and Usage of the Reaction Path Concept. In D. Heidrich, editor, *The Reaction Path in Chemistry: Current Approaches and Perspectives*, pages 1–10. Kluwer Academic Publishers, 1995.
3. W. Quapp and D. Heidrich. Analysis of the concept of minimum energy path on the potential energy surface of chemically reacting systems. *Theor Chim Acta*, 66:245–260, 1984.
4. K. Fukui. A Formulation of the Reaction Coordinate. *J Phys Chem*, 74:4161–4163, 1970.
5. M. Hirsch and W. Quapp. The reaction pathway of a potential energy surface as curve with induced tangent. *Chem Phys Lett*, 395:150–156, 2004.
6. J. Pancíř. Calculation of the least energy path on the energy hypersurface. *Collection Czechoslov Chem Commun*, 40:1112–1118, 1975.
7. M.V. Basilevsky and A.G. Shamov. The local definition of the optimum ascent path on a multi-dimensional potential energy surface and its practical application for the location of saddle points. *Chemical Physics*, 60:347–358, 1981.
8. D.K. Hoffman, R.S. Nord, and K. Ruedenberg. Gradient Extremals. *Theor Chim Acta*, 69:265–279, 1986.
9. D. Heidrich, W. Kliesch, and W. Quapp. *Properties of Chemically Interesting Potential Energy Surfaces*, volume 56 of *Lecture Notes in Chemistry*. Springer, 1991.
10. J.-Q. Sun and K. Ruedenberg. Gradient Extremals and steepest descent lines on potential energy surfaces. *J Chem Phys*, 98:9707–9714, 1993.
11. W. Quapp, O. Imig, and D. Heidrich. Gradient Extremals and their Relation to the Minimum Energy Path. In D. Heidrich, editor, *The Reaction Path in Chemistry: Current Approaches and Perspectives*, pages 137–160. Kluwer Academic Publishers, 1995.

12. S. Perković, E.M. Blokhuis, E. Tessler, and B. Widom. Boundary tension: From wetting transition to prewetting critical point. *J Chem Phys*, 102:7584–7594, 1995.
13. W. Quapp, M. Hirsch, O. Imig, and D. Heidrich. Searching for Saddle Points of Potential Energy Surfaces by Following a Reduced Gradient. *J Comput Chem*, 19:1087–1100, 1998.
14. J.M. Bofill and J.M. Anglada. Finding transition states using reduced potential-energy surfaces. *Theor Chem Acc*, 105:463–472, 2001.
15. R. Crehuet, J.M. Bofill, and J.M. Anglada. A new look at the reduced-gradient-following path. *Theor Chem Acc*, 107:130–139, 2002.
16. W. Quapp. Reduced Gradient Methods and their Relation to Reaction Paths. *J Theor Comput Chem*, 2:385–417, 2003.
17. P. Valtazanos and K. Ruedenberg. Bifurcations and transition states. *Theor Chim Acta*, 69:281–307, 1986.
18. W. Quapp. How does a reaction path branching take place? A classification of bifurcation events. *J Molec Struct*, 695–696:95–101, 2004.
19. W. Quapp, J.M. Bofill, and A. Aguilar-Mogas. Exploration of cyclopropyl radical ring opening to allyl radical by Newton trajectories: importance of valley-ridge inflection points to understand the topography. *Theor Chem Acc*, 129:803–821, 2011.
20. H.Th. Jongen, P. Jonker, and F. Twilt. *Nonlinear Optimization in* $\mathbb{R}^n$, volume 32 of *Methoden und Verfahren der Mathematischen Physik*. Peter Lang, 1983.
21. I. Diener. *Globale Aspekte des kontinuierlichen Newtonverfahrens*. Habilitation, Göttingen, 1991.
22. V. Bakken, D. Danovich, S. Shaik, and H.B. Schlegel. A Single Transition State Serves Two Mechanisms: An ab Initio Classical Trajectory Study of the Electron Transfer and Substitution Mechanisms in Reactions od Ketyl Radical Anions with Alkyl Halides. *J Am Chem Soc*, 123:130–134, 2001.
23. D.H. Ess, S.E. Wheeler, R.G. Iafe, L. Xu, N. Çelebi-Ölçüm, and K.N. Houk. Bifurcations on Potential Energy Surfaces of Organic Reactions. *Angew Chem Int Ed*, 47:7592–7601, 2008.
24. J.B. Thomas, J.R. Waas, M. Harmata, and D.A. Singleton. Control Elements in Dynamically Determined Selectivity on a Bifurcating Surface. *J Am Chem Soc*, 130:14544–14555, 2008.
25. W. Quapp. General discussion. *J Chem Soc, Faraday Trans*, 90:1607–1608, 1994.
26. H.B. Schlegel. Some thoughts on reaction-path following. *J Chem Soc, Faraday Trans*, 90:1569–1574, 1994.
27. W. Quapp, M. Hirsch, and D. Heidrich. Bifurcation of reaction pathways: the set of valley ridge inflection points of a simple three-dimensional potential energy surface. *Theor Chem Acc*, 100:285–299, 1998.
28. W. Quapp. Chemical Reaction Paths and Calculus of Variations. *Theor Chem Acc*, 121:227–237, 2008.
29. J.M. Bofill. Is the reduced gradient following path a curve with extremal properties? *J Chem Phys*, 130:176102, 2009.
30. J.M. Bofill and W. Quapp. Variational nature, integration, and properties of Newton reaction path. *J Chem Phys*, 134:074101, 2011.
31. M. Hirsch, W. Quapp, and D. Heidrich. The set of valley-ridge inflection points on the potential energy surface of water. *Phys Chem Chem Phys*, 1:5291–5299, 1999.
32. W. Quapp and V. Melnikov. Valley-Ridge-Inflection Points of the Potential Energy Surface of H_2S, H_2Se, and H_2CO. *Phys Chem Chem Phys*, 3:2735–2741, 2001.
33. W. Quapp, M. Hirsch, and D. Heidrich. An approach to reaction path branching using valley-ridge inflection points of potential energy surfaces. *Theor Chem Acc*, 112:40–51, 2004.
34. W. Quapp and B. Schmidt. An empirical, variational method of approach to unsymmetric valley-ridge inflection points. *Theor Chem Acc*, 128:47–61, 2011.
35. F.H. Branin. Widely convergent methods for finding multiple solutions of simultaneous nonlinear equations. *IBM J Res Develop*, 16:504–522, 1972.
36. J.M. Ortega and W.C. Rheinboldt. *Iterative solution of nonlinear equations in several variables*. Academic Press, 1970.
37. A. Ben-Israel and T.N.E. Greville. *Generalized Inverses: Theory and Applications*. John Wiley, 1974.
38. E.L. Allgower and K. Georg. Numerical path following. In P.G. Ciarlet and J.L. Lions, editors, *Handbook of Numerical Analysis*, volume 5, pages 3–207. North-Holland, 1997.
39. W.H. Press, S.A. Teukolsky, W.T. Vetterling, and B.P. Flannery. *Numerical Recipes in Fortran 77: The Art of Scientific Computing*. Cambridge University Press, 2nd edition, 1992.
40. A.A. Granovsky. Firefly Version 7.1.G. `http://classic.chem.msu.su/gran/firefly/index.html`.
41. I. Diener and R. Schaback. An Extended Continuous Newton Method. *Journal of Optimization Theory and Applications*, 67:57–77, 1990.